



Cite this: *Chem. Commun.*, 2024, 60, 14597

Received 7th October 2024,
Accepted 11th November 2024

DOI: 10.1039/d4cc05273k

rsc.li/chemcomm

Machine learning directed discovery and optimisation of a platinum-catalysed amide reduction†

Eleonora Casillo,^a Benon P. Maliszewski,^{ID, a} César A. Urbina-Blanco,^{ID, bc} Thomas Scattolin,^{ID, d} Catherine S. J. Cazin^{ID, *a} and Steven P. Nolan^{ID, *a}

The discovery and optimisation of reaction conditions leading to the reduction of amides, a fundamental large-scale industrial reaction, is achieved using a machine learning (ML) platform and a platinum catalyst. The optimisation leads to the discovery of a new platinum-based catalytic system that displays unexpectedly high performance. The approach enables rapid and high conversions at ppm-level catalyst loadings.

The optimisation of chemical reactions traditionally relies on empirical methods, where chemists adjust parameters based on their understanding to achieve optimal outcomes. This approach is time-consuming and resource-intensive, often involving trial-and-error experimentation.¹ Machine learning (ML) excels at extracting implicit knowledge from data by inferring functional relationships statistically, even without detailed problem-specific knowledge.² Unlike traditional approaches, ML starts from a generalised model and iteratively refines it, enabling early exploration of problems. Combining data-driven algorithms with scientific theories is increasingly common, generating novel insights and applications.³ This interdisciplinary approach enhances the synergy between data-driven methods and theoretical frameworks, deepening our understanding of complex systems. We have deployed an intuitive ML platform accessible *via* a web browser,⁴ an algorithm that has been developed to reduce the number of trials for chemical process optimisation, while providing performance predictions and recommendations to minimise uncertainty. Applying such models to industrially

significant chemical reactions is a current and promising challenge, as it enables cost reduction, improved efficiency, and decreased carbon emissions, time, energy consumption, and raw material use.

Amines are one of the most important classes of molecules in organic synthesis, especially in scaffolds making up active ingredients of natural products, pharmaceuticals, and agrochemicals. They also play a crucial role in the production of bulk and fine chemicals, contributing to the manufacturing of plastics, textiles, surfactants, dyes, and various other products of everyday life.⁵ Their importance extends to a wide range of applications,⁶ including commonly used drugs such as morphine, ephedrine, and amoxapine, as well as cosmetics such as shampoos and soaps. Consequently, the development of innovative methodologies for constructing complex amine architectures remains a key focus in organic synthesis.

In this work, we aim to leverage the vast potential of ML algorithms to optimise the platinum-catalysed reduction of amides to amines under hydrosilylation conditions (Fig. 1).

The reduction of amides can be categorised into two primary types: (i) the complete reduction to amine compounds and (ii) the reduction yielding a mixture of alcohols and amines.⁷ The direct reduction of amides to amines often requires very reactive reagents such as LiAlH₄ or NaBH₄, which possess several limitations and practical safety and reactivity disadvantages. For these reasons, catalytic systems using molecular hydrogen or hydrosilanes have shown promise in enhancing efficiency and selectivity in this transformation. Key developments include Ito's and Harrod's approaches using diphenylsilane or methylphenylsilane as a reducing agents (Fig. 1A and B).⁸ Notably, Vaska's complex $[\text{IrCl}(\text{CO})(\text{PPh}_3)_2]$ ⁹ with 1,1,3,3-tetramethyldisiloxane (TMDS) has demonstrated exceptional efficiency and selectivity in the hydrosilylation of tertiary amides.⁶ Despite these advances, amides remained challenging substrates until the early 2000s, when new catalysts based on Co, Cu, Fe, Mo, Rh, Ru, and Zn emerged. In 2009, Nagashima and colleagues showed that a triruthenium cluster, $[(\mu^3, \eta^2, \eta^3, \eta^5\text{-acenaphthylene})\text{Ru}_3(\text{CO})_7]$,

^a Department of Chemistry and Center for Sustainable Chemistry, Ghent University, Krijgslaan 281 (S-3), 9000 Ghent, Belgium. E-mail: catherine.cazin@ugent.be, steven.nolan@ugent.be

^b Sunthetics, 3055 Hunter Rd, San Marcos, TX 78666, USA

^c Prophecy Labs, Raymond Blyckaerts 13, Ixelles, 1050, Belgium

^d Dipartimento di Scienze Chimiche, Università degli Studi di Padova, via Marzolo 1, 35131 Padova, Italy

† Electronic supplementary information (ESI) available: Experimental procedures, characterisation data and NMR spectra. See DOI: <https://doi.org/10.1039/d4cc05273k>



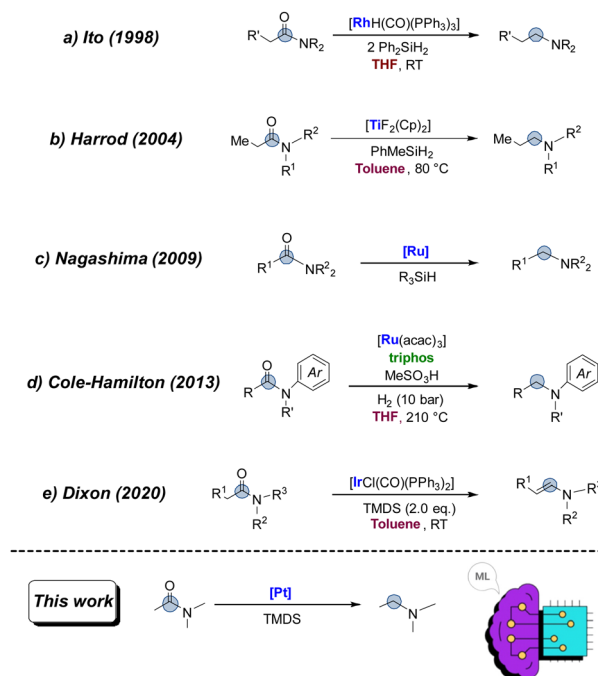


Fig. 1 Examples of transition metal-catalysed reduction of amides and our discovery/optimisation via a machine learning algorithm.

efficiently catalyses the reduction of tertiary amides with hydrosilanes (Fig. 1C).¹⁰ Four years later, Cole-Hamilton reported the deoxygenative hydrogenation of amides catalysed by $[\text{Ru}(\text{acac})_3]$ and triphos with methanesulfonic acid (Fig. 1D).¹¹ Since this breakthrough, numerous research groups have devised metal-mediated hydrosilylation employing various metals like Ru,¹² Zn,¹³ Pt,¹⁴ Mn,¹⁵ Ir¹⁶ and Ni.¹⁷ In 2009, Nagashima and co-workers used commercially available and inexpensive TMDS, which is a practically useful reductant, and several Pt compounds as catalysts such as $\text{H}_2\text{PtCl}_6 \cdot 6\text{H}_2\text{O}$, $[\text{Pt}(\text{dba})_2]$, $[\text{Pt}(\text{cod})\text{Cl}_2]$ and Pt/C .¹⁴ Although silanes are generally unreactive and require activators to function as reducing agents in the catalytic cycle, the integration of precious metal-based catalysts with various ligands

has proven effective for the efficient reduction of amides.¹¹ Notably, the reduction of carbonyl compounds with silanes under acidic conditions has been recognised since the 1970s.¹⁸ Given the greater ease of handling hydrosilanes compared to traditional hydride-based reagents, the current platinum-catalysed reduction of amides with hydrosilanes deserves further attention, especially when the reaction can be adapted for large-scale production of amines.

Nagashima's key discovery of the 'dual Si-H effect' showed that using silanes with two adjacent Si-H groups can significantly accelerate the reduction of amides to amines when using a platinum-based catalyst.¹⁴ In fact, a significant acceleration of the reaction rate is observed when using hydrosilanes containing two adjacent Si-H groups, achieving results that are unattainable with standard mono-hydrosilanes under mild conditions.

In this work, two types of catalyst were used: two thioether-Pt(II)-based and three NHC-Pt(II)-based. Recently, Markó and co-workers achieved excellent results with Pt(0)-N-heterocyclic carbene complexes as hydrosilylation pre-catalysts.¹⁹ It is noteworthy that Pt(II)-NHC catalysts exhibit a high stability under the reaction conditions, due to the strength of the NHC-Pt bond, which limits the formation of [Pt] colloids during the benchmark hydrosilylation reactions.^{19,20} On the other hand, the two simply accessible thioether complexes exhibit stability in air and moisture, which renders them easy to handle, while achieving high efficiencies.²¹

In this project, we propose a ML-guided reduction of *N,N*-dimethylacetamide using TMDS as the reducing agent and the five different platinum-based catalysts. First, the Sunthetics platform allows users to select the number and type of reaction conditions they wish to monitor and modify across different experiments. In this case, the algorithm controls three key variables: (i) reaction time, ranging from 1 to 24 hours; (ii) temperature, set between room temperature (25 °C) and 80 °C; (iii) catalyst loading, from a minimum of 0.01 mol% to a maximum of 1.00 mol%. After each reaction, the algorithm evaluates the experimentally obtained conversion, turnover frequency (TOF), and turnover number (TON), to identify what

Table 1 First set of 10 reactions suggested by the machine learning algorithm

Entry ^a	[Pt]	Cat. loading (mol%)	Time (h)	T (°C)	Conversion (%)	TON	TOF (h ⁻¹)
1	$[\text{Pt}(\text{DMS})_2\text{Cl}_2]^b$	1.00	21	RT	NR	—	—
2	$[\text{Pt}(\text{DMS})_2\text{Cl}_2]$	0.70	7	30	>99	141	20
3	$[\text{Pt}(\text{ICy})(\text{DMS})\text{Cl}_2]$	1.00	2	50	48	48	24
4	$[\text{Pt}(\text{IMes})(\text{DMS})\text{Cl}_2]$	0.50	22	70	60	120	5
5	$[\text{Pt}(\text{SIPr})(\text{DMS})\text{Cl}_2]$	0.80	18	50	36	45	2
6	$[\text{Pt}(\text{DMS})_2\text{Cl}_2]$	0.15	3	34	>99	667	222
7	$[\text{Pt}(\text{ICy})(\text{DMS})\text{Cl}_2]$	0.35	2	60	NR	—	—
8	$[\text{Pt}(\text{IMes})(\text{DMS})\text{Cl}_2]$	0.55	23	66	52	94	4
9	$[\text{Pt}(\text{SIPr})(\text{DMS})\text{Cl}_2]$	0.95	7	40	30	31	4
10	$[\text{Pt}(\text{THT})_2\text{Cl}_2]$	0.50	20	50	>99	200	10

^a Reaction conditions: *N,N*-dimethylacetamide: 0.5 mmol; 1,1,3,3-tetramethyldisiloxane: 1.5 mmol. ^b PHMS 1.5 mmol.



it predicts to be the optimal conditions. It then adjusts the values of these three variables, suggesting subsequent reactions with modified temperature, time, and catalyst loading.

Table 1 presents the first ten reactions proposed by the algorithm. Notably, the first reaction was conducted using PHMS (polymethylhydrosiloxane) instead of TMDS, due to its low cost as a byproduct of the silicone industry. However, this approach was unsuccessful, as PHMS tends to cross-link and solidify in the presence of a platinum-based catalyst, resulting in no conversion to the desired product (Table 1, entry 1).

Excluding entry 1, with only nine experiments, that also differ in the type of catalyst used, complete conversion of the substrate was achieved in three cases (entries 2, 6, and 10), with TON values ranging from 141 to 667. Based on the analysis of these promising results, the algorithm generated a refined set of new reactions to be performed, with the variables adjusted to maximise the outcomes. The reaction conditions and the corresponding results are presented in Table 2, which includes the next two sets of reactions proposed by the algorithm (first set, entries 1–5; second set, entries 6–10).

In addition to predicting new sets of efficient reactions, the algorithm simultaneously provides several outputs, including correlation graphs between the selected variables and outputs (Fig. 2). The correlation graph illustrates the relationship between the variables and the target, revealing a correlation coefficient of 0.94 between TOF and TON.

Interpreting the values obtained from the initial analyses reported in Table 1, it can be immediately inferred that $[\text{Pt}(\text{DMS})_2\text{Cl}_2]$ and $[\text{Pt}(\text{THT})_2\text{Cl}_2]$ appear to be the most effective catalysts for this reaction. Among the first ten reactions suggested by the algorithm, the reaction employing $[\text{Pt}(\text{DMS})_2\text{Cl}_2]$ (0.15 mol%) at 34 °C exhibited the highest performance, achieving total conversion after 3 hours (entry 6, Table 1). Another highly promising result emerged from the initial tests with $[\text{Pt}(\text{THT})_2\text{Cl}_2]$ (0.50 mol%), which led to complete substrate conversion after 20 hours at 50 °C

Table 2 Next sets of reactions suggested by the algorithm and catalytic outcomes

Entry	Catalyst	Cat. (mol%)	t (h)	T (°C)	Conv. (%)	TOF (h ⁻¹)
1	$[\text{Pt}(\text{DMS})_2\text{Cl}_2]$	0.15	3	33	>99	222
					>99 ^a	333
2	$[\text{Pt}(\text{DMS})_2\text{Cl}_2]$	0.14	17	36	>99	42
					>99 ^a	357
3	$[\text{Pt}(\text{DMS})_2\text{Cl}_2]$	0.01	15	39	>99	667
					>99 ^a	5002
4	$[\text{Pt}(\text{IMes})(\text{DMS})\text{Cl}_2]$	0.13	14	36	NR	—
5	$[\text{Pt}(\text{ICy})(\text{DMS})\text{Cl}_2]$	1.00	21	70	>99	5
					36 ^a	
6	$[\text{Pt}(\text{DMS})_2\text{Cl}_2]$	0.03	20	38	83	138
7	$[\text{Pt}(\text{DMS})_2\text{Cl}_2]$	0.05	20	39	>99 ^b	100
8	$[\text{Pt}(\text{DMS})_2\text{Cl}_2]$	0.03	16	50	46	96
9	$[\text{Pt}(\text{ICy})(\text{DMS})\text{Cl}_2]$	0.01	18	70	NR	—
10	$[\text{Pt}(\text{THT})_2\text{Cl}_2]$	0.45	14	37	>99 ^b	16

^a Monitored by ¹H NMR after 2 hours. ^b Conversion already at >99% after 1 hour.

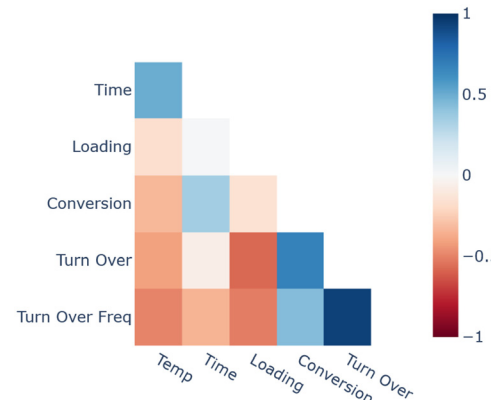


Fig. 2 Correlation graph between inputs and outputs.

(entry 10, Table 1). In the subsequent set of five reactions (see Table 2), the best performance was again achieved using $[\text{Pt}(\text{DMS})_2\text{Cl}_2]$ as the catalyst. Although the algorithm suggested specific reaction times, additional experiments were conducted with a standardised time of 2 hours to monitor reaction progress.

Notably, complete conversion was achieved within 2 hours for the first three entries in Table 2, despite the algorithm recommending longer reaction times of 3, 17, and 15 hours, respectively.

Upon confirming the high performance of the thioether-based catalysts, efforts were made to minimise the catalytic charges. The optimal result was obtained with $[\text{Pt}(\text{DMS})_2\text{Cl}_2]$ (0.01 mol%) at 39 °C, achieving complete conversion after 2 hours (entry 3, Table 2), with a turnover frequency (TOF) of 5002 h⁻¹ (the highest value recorded). Another notable outcome was the reaction using $[\text{Pt}(\text{THT})_2\text{Cl}_2]$ at 0.45 mol% and 37 °C, which resulted in complete conversion after just one hour (entry 10, Table 2).

Between the two catalysts, while both demonstrated rapid and efficient performance, $[\text{Pt}(\text{DMS})_2\text{Cl}_2]$ enabled similar results with significantly lower quantities, making it the optimal choice for reaction optimisation. For the sake of completeness, several additional reactions not recommended by the algorithm were conducted. As data from these reactions became available, new considerations and reaction conditions were devised based on chemical reasoning, including experiments at room temperature (RT, 25 °C), a condition not previously recommended by the algorithm. The results of these experiments are summarised in Table 3. Two reactions are particularly noteworthy: the first (entry 1) using $[\text{Pt}(\text{DMS})_2\text{Cl}_2]$ at 0.13 mol% at RT, and the second (entry 6) using $[\text{Pt}(\text{THT})_2\text{Cl}_2]$ at 0.45 mol% at RT. In the first case, substrate conversion reached 92% within one hour, although the rate slowed, achieving complete conversion after 24 hours.

In conclusion, with the valuable assistance of the Sunthetics ML platform, we identified the optimal condition for the reduction of *N,N*-dimethylacetamide to dimethylethylamine using $[\text{Pt}(\text{DMS})_2\text{Cl}_2]$ as catalysts with a 0.01 mol% loading. Complete substrate conversion was achieved under extremely mild conditions (2 hours, 39 °C) and without the use of a solvent, reaching a TOF of 5002 h⁻¹.

The algorithm proved highly effective for optimisation, accelerating the reaction conditions discovery process and reducing material usage compared to traditional methods.



Table 3 Set of reactions not suggested by the algorithm and results

Entry	Catalyst	Cat. loading (mol%)	T (°C)	Conversion (%)							TOF (h ⁻¹) ^a
				1 h	2 h	4 h	6 h	8 h	24 h		
1	[Pt(DMS) ₂ Cl ₂]	0.13	RT	92	94	95	96	97	>99	708	
2	[Pt(IMes)(DMS)Cl ₂]	0.40	70	22	26	29	32	34	45	55	
3	[Pt(ICy)(DMS)Cl ₂]	0.40	50	19	22	36	44	49	>99	48	
4	[Pt(DMS) ₂ Cl ₂]	0.03	RT	44	45	46	50	51	54	1467	
5	[Pt(DMS) ₂ Cl ₂]	0.05	RT	20	26	29	33	36	38	400	
6	[Pt(THT) ₂ Cl ₂]	0.45	RT	>99	—	—	—	—	—	222	

^a Calculated after 1 hour.

This approach, when combined with operator expertise, holds great promise for delivering significant results, even in more complex reactions involving multiple variables. Although this study focused on a single substrate to facilitate optimisation, expanding the method to other substrates becomes an iterative process that can also be automated. Further investigations into the nature of the silane could also lead to improving reaction efficiency. As with any robust predictive model, the margin of error has been quantified by generating an error graph for each variable (see Fig. S2 in ESI[†]). This graphical representation illustrates the relationship between observed values and the corresponding obtained ones. Upon examining the distribution of obtained values, it is evident that they closely align with the trend drawn by the predicted values. This observation suggests a strong correlation, indicative of a well-functioning model. This study highlights the significant synergy that can be established between scientists and machines. Specifically, the integration of human intuition with the Sunthetics tool enabled rapid and efficient discovery and optimisation.

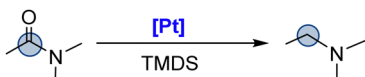
This project received support from the iBOF-project C3 (01IB1020). The FWO is acknowledged for a PhD fellowship to B. P. M. (1SB5321N) and for senior research grants to SPN (G0A6823N) and CSJC (G0C5423N). Umicore AG are thanked for generous gifts of materials.

Data availability

Additional data supporting this article have been included as part of the ESI.[†]

Conflicts of interest

Sunthetics LLC is a commercial developer and provider of the SuntheticsML algorithm. CAUB was a Sunthetics contractor at the time of the study.



Notes and references

- P. M. Murray, S. N. Tyler and J. D. Moseley, *Org. Process Res. Dev.*, 2013, **17**, 40–46.
- I. H. Sarker, *SN Comput. Sci.*, 2021, **2**, 160.
- D. Frey, J. H. Shin, C. Musco and M. A. Modestino, *React. Chem. Eng.*, 2022, **7**, 855–865.
- “Sunthetics - Accelerating innovation in the chemical industry with AI,” can be found under <https://sunthetics.io/>.
- V. Froidevaux, C. Negrell, S. Caillol, J.-P. Pascault and B. Boutevin, *Chem. Rev.*, 2016, **116**, 14181–14224.
- D. Matheau-Raven, P. Gabriel, J. A. Leitch, Y. A. Almehmadi, K. Yamazaki and D. J. Dixon, *ACS Catal.*, 2020, **10**, 8880–8897.
- Z. Wang, Y. Li, Q. Liu, G. A. Solan, Y. Ma and W. Sun, *ChemCatChem*, 2017, **9**, 4275–4281.
- R. Kuwano, M. Takahashi and Y. Ito, *Tetrahedron Lett.*, 1998, **39**, 1017–1020.
- L. Vaska and J. W. DiLuzio, *J. Am. Chem. Soc.*, 1961, **83**, 2784–2785.
- K. Matsubara, T. Iura, T. Maki and H. Nagashima, *J. Org. Chem.*, 2002, **67**, 4985–4988.
- J. Coetzee, D. L. Dodds, J. Klankermayer, S. Brosinski, W. Leitner, A. M. Slawin and D. J. Cole-Hamilton, *Chem. – Eur. J.*, 2013, **19**, 11039–11050.
- S. Hanada, T. Ishida, Y. Motoyama and H. Nagashima, *J. Org. Chem.*, 2007, **72**, 7551–7559.
- S. Das, D. Addis, S. Zhou, K. Junge and M. Beller, *J. Am. Chem. Soc.*, 2010, **132**, 1770–1771.
- S. Hanada, E. Tsutsumi, Y. Motoyama and H. Nagashima, *J. Am. Chem. Soc.*, 2009, **131**, 15032–15040.
- C. M. Kelly, R. McDonald, O. L. Sydora, M. Stradiotto and L. Turculet, *Angew. Chem., Int. Ed.*, 2017, **56**, 15901–15904.
- C. Cheng and M. Brookhart, *J. Am. Chem. Soc.*, 2012, **134**, 11304–11307.
- B. J. Simmons, M. Hoffmann, J. Hwang, M. K. Jackl and N. K. Garg, *Org. Lett.*, 2017, **19**, 1910–1913.
- M. P. Doyle, D. J. DeBruyn and D. A. Kooistra, *J. Am. Chem. Soc.*, 1972, **94**, 3659–3661.
- I. E. Marko, S. Sterin, O. Buisine, G. Mignani, P. Branlard, B. Tinant and J.-P. Declercq, *Science*, 2002, **298**, 204–206.
- B. P. Maliszewski, T. A. C. A. Bayrakdar, P. Lambert, L. Hamdouna, X. Trivelli, L. Cavallo, A. Poater, M. Beliš, O. Lafon, K. Van Hecke, D. Ormerod, C. S. J. Cazin, F. Nahra and S. P. Nolan, *Chem. – Eur. J.*, 2023, **29**, e202301259.
- B. P. Maliszewski, E. Casillo, P. Lambert, F. Nahra, C. S. J. Cazin and S. P. Nolan, *Chem. Commun.*, 2023, **59**, 14017–14020.

